Research Article

Neural stem cell transplantation alleviates functional cognitive deficits in a mouse model of tauopathy

https://doi.org/10.4103/1673-5374.314324
Date of submission: November 2, 2020
Date of decision: December 17, 2020
Date of acceptance: February 23, 2021
Date of web publication: June 7, 2021

He-Ao Zhang, Chun-Xu Yuan, Ke-Fu Liu, Qi-Fan Yang, Juan Zhao, Hui Li, Qing-Hu Yang, Da Song, Zhen-Zhen Quan*, Hong Qing*

Graphical Abstract *NSCs transplantation is comprehensively involved in the brain function to perform its role in AD treatment*

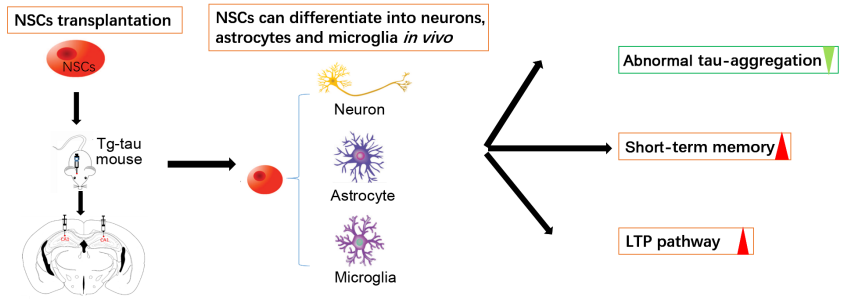

Abstract

The mechanisms of the transplantation of neural stem cells (NSCs) in the treatment of Alzheimer's disease remain poorly understood. In this study, NSCs were transplanted into the hippocampal CA1 region of the rTg (tau P301L) 4510 mouse model, a tauopathy model that is thought to reflect the tau pathology associated with Alzheimer's disease. The results revealed that NSC transplantation reduced the abnormal aggregation of tau, resulting in significant improvements in the short-term memory of the tauopathy model mice. Compared with wild-type and phosphate-buffered saline (PBS)-treated mice, mice that received NSC transplantations were characterized by changes in the expression of multiple proteins in brain tissue, particularly those related to the regulation of tau aggregation or misfolding. Kyoto Encyclopedia of Genes and Genomes (KEGG) pathway analysis and Gene Ontology (GO) function analysis revealed that these proteins were primarily enriched in pathways associated with long-term potentiation, neurogenesis, and other neurobiological processes. Changes in the expression levels of key proteins were verified by western blot assays. These data provided clues to improve the understanding of the functional capacity associated with NSC transplantation in Alzheimer's disease treatment. This study was approved by the Beijing Animal Ethics Association and Ethics Committee of Beijing Institute of Technology (approval No. SYXK-BIT-school of life science-2017-M03) in 2017.
Key Words: Alzheimer's disease; cell transplantation; neural differentiation; neural stem cells; proteomic analysis; short-term memory; tauopathy

Chinese Library Classification No. R456; R741; Q421

Introduction

Owing to the self-renewal and pluripotent capacity of stem cells, which are able to differentiate into various cell types, stem cell therapy has been viewed as a potential therapeutic strategy that could be applied to a variety of diseases, including ischemic stroke, spinal cord injury, and central nervous system diseases, such as Alzheimer's disease (AD), Parkinson's disease, and Huntington's disease (Gonzalez et al., 2016; Yousefifard et al., 2016; Bernstock et al., 2017). One of the most common neurodegenerative diseases worldwide, AD is pathologically characterized by the formation of β-amyloid (Aβ) plaques, neurofibrillary tangles (NFTs), and neurodegeneration, resulting in synaptic loss, neuronal dysfunction, and death (Li et al., 2014). Diverse mechanisms are involved in the development of AD, increasing the difficulty of developing effective AD treatments, and thus far, no effective therapies have been developed to cure AD.

With the development of stem cell therapies, attempts to promote the repair and regeneration of impaired neural circuitry using endogenous stem cells are becoming an increasingly prevalent therapeutic strategy. Neural stem cells (NSCs), which are found in the brains of mammals, are able to differentiate into several types of neural cells, including neurons and glial cells (Kang et al., 2016; Cosacak et al., 2020; Ji et al., 2020). Induced human neuronal cells have been shown to be homogeneous, capable of stably expressing various neural-specific proteins, generating action potentials, and forming functional synapses (Pang et al., 2011; Kang et al., 2016). Stem cell transplantations targeted to the fimbria fornix were able to improve cognition in the APPswe/PS1deltaE9

Key Laboratory of Molecular Medicine and Biotherapy, School of Life Science, Beijing Institute of Technology, Beijing, China
*Correspondence to: Zhen-Zhen Quan, PhD, qzzbit2015@bit.edu.cn; Hong Qing, PhD, hqing@bit.edu.cn.
https://orcid.org/0000-0001-6097-3240 (He-Ao Zhang); https://orcid.org/0000-0002-2557-0371 (Zhen-Zhen Quan); https://orcid.org/0000-0003-2820-450X (Hong Qing)

Funding: *This work was supported by the National Key Research and Development Program of China, Nos. 2017YFE0117000 (to ZZQ), 2018YFC1312302-3 (to HQ); the Beijing Advanced Innovation Center for Intelligent Robots and Systems of China, No. 2018IRS12 (to ZZQ); and the National Natural Science Foundation of China, Nos. 82001167 (to HL), 81870844 (to HQ), 81701260 (to ZZQ).*
How to cite this article: *Zhang HA, Yuan CX, Liu KF, Yang QF, Zhao J, Li H, Yang QH, Song D, Quan ZZ, Qing H (2022) Neural stem cell transplantation alleviates functional cognitive deficits in a mouse model of tauopathy. Neural Regen Res 17(1):152-162.*

(referred to as APP/PS1) murine model, a double transgenic AD mouse model featuring mutations in two AD-associated proteins, which was accompanied by a reduction in Aβ plaque development and the increased recruitment of activated microglia to the hippocampal and cortical regions (McGinley et al., 2018). Previously, human NSC engraftment was shown to improve cognition in two complementary models (3×Tg-AD and CaM/Tet-DTA mice) of neurodegeneration by enhancing endogenous synaptogenesis without affecting Aβ or tau pathology (Ager et al., 2015). This finding was consistent with those from other studies reporting that hippocampal NSC transplantation could rescue spatial learning and memory deficits in aged 3×Tg-AD mice through effects on brain-derived neurotrophic factor (BDNF) rather than through changes in Aβ/tau pathology (Blurton-Jones et al., 2009). Evidence has suggested that the transplantation of human NSCs could restore cognitive dysfunction in APP/PS1 model mice, which was thought to be mediated by improvements in neuronal connectivity and metabolic activity (Li et al., 2016). Thus, exploring the application of NSC transplantation in AD treatment appears to be both promising and intriguing and might provide important cues for clinical studies.

We, therefore, proposed to transplant NSCs into a transgenic mouse model of AD to examine the effects on cognitive functions and AD pathology. We investigated the molecular changes that occurred in response to NSC transplantation to further explore the functional effects of NSC transplantation in AD treatment.

Materials and Methods

Animals

For this study, rTg (tau P301L) 4510 mice (referred to as Tg-tau mice) were obtained through the hybridization between transgenic tau mice (FVB, gifted by the Xuanwu Hospital in Beijing, China) and the transgenic Tta mice (C57BL/6, purchased from the Jackson Laboratory, Bar Harbor, ME, USA). Twenty-two Tta^+/Tau^+ mice (40 weeks old) were randomly selected from among the hybridized offspring and randomly separated into two groups: NSC-transplanted (Tg + NSCs; n = 11) and phosphate-buffered saline (PBS)-treated (Tg + PBS; n = 11) groups. Six Tta^-/Tau^- double negative mice (40 weeks old) were randomly selected as the control group. The mice were allowed to adapt to the environment for approximately 5 days prior to experiments and were provided with food and water ad libitum under standard housing conditions, at a room temperature of 23 ± 2°C, 12-hour light/dark cycle, and humidity of 40–60%. No more than four mice were housed in each standard cage. All animal experiments were performed in accordance with the Guidelines of the Beijing Animal Ethics Association, and the Ethics Committee of Beijing Institute of Technology (approval No. SYXK-BIT-school of life science-2017-M03) approved the study in 2017.

Extraction of primary NSCs

Primary NSCs were extracted from the hippocampus of C57BL/6 wild-type (WT) suckling mice on postnatal day 1 (purchased from the Department of Laboratory Animal Science, Peking University Medical School, Beijing, China, license No. SCXK (Jing) 2016-0010). The experimental details are as follows: the newborn mouse was paralyzed and anesthetized by cooling on ice, and the brain was separated from the skull and maintained in PBS. The hippocampus (Song et al., 2018) was separated from the brain under a microscope (Zoom 2380; WUMO, Shanghai, China) and sliced into pieces using tweezers. One milliliter of 0.25% trypsin (Cat#T1300; Solarbio, Beijing, China) was added to the sliced hippocampus, spread evenly, and placed in a 37°C incubator for 15 minutes. One milliliter of PBS buffer was added to dilute the trypsin and mixed by repeated pipetting, and the mixture was transferred to a 15 mL centrifuge tube and centrifuged at 2500 r/min for 5 minutes. The supernatant was discarded, the cells were suspended in complete medium (Dulbecco's modified Eagle medium:F-12 [DMEM/F12; Gibco, Thermo Fisher, Waltham, MA, USA], 2% B27 [Gibco], 0.02% fibroblast growth factor-basic [bFGF] stock [PeproTech, Rocky Hill, NJ, USA], 0.01% epidermal growth factor [EGF] stock [PeproTech], and 1% penicillin-streptomycin mixture [Solarbio]), and the cell suspension was filtered through a 200-mesh cell sieve to obtain primary cells. The primary cells were cultured with 10 mL of complete medium in a medium-sized dish (60 mm × 15 mm, Corning, Corning, NY, USA) and incubated at 37°C. After 12 hours, half of the completed medium was removed and replaced with the same volume of fresh complete medium, which was repeated every 3 days. The cells were passaged from P0 to P3 every 7 days via accutase digestion. The NSCs were observed by an inverted microscope (IX71, Olympus, Tokyo, Japan).

Cell transfection

The third generation of *in vitro* primary NSC cultures were transfected with a lentivirus-green fluorescent protein (GFP) virus (CMVGFP, Cyagen Biosciences, Guangzhou, China) at multiplicity of infection (MOI) values of 5, 10, and 20. Stem cell spheres in the logarithmic growth phase were digested with accutase (Sigma, New York, NY, USA) to prepare a single-cell suspension, which was seeded into a new medium-sized dish (60 mm × 15 mm, Corning) at a density of 3.0×10^6 cells/dish in anti-antibiotic complete medium. On the basis of the results of the preliminary experiment, an MOI of 20 was selected for transfection, and the virus titer was 8.85×10^8. Using the formula (MOI × cell number × 10^3)/(8.85×10^8), 67.8 μL of the lentivirus-GFP was added to the media. After 12 hours of transfection, fresh anti-antibiotic complete media was added, and fluorescence was viewed under an inverted microscope.

In vitro NSC differentiation and immunofluorescence

The NSCs transfected with lentivirus-GFP were cultured *in vitro*, and their differentiation potential was observed via the detection of the green fluorescence expression. Polylysine (10×, Solarbio) was diluted with sterile water and used to coat a confocal dish (NEST Biotechnology Co. Ltd., Wuxi, China) at 37°C overnight. The liquid was discarded, and the plate was washed three times with sterile water for 5 minutes each time. The confocal dishes were sealed with parafilm and stored at 4°C until use. An NSC suspension was collected, centrifuged, resuspended in differentiation medium (DMEM/F12, 10% fetal bovine serum), plated onto polylysine-coated confocal dishes, and cultured at 37°C, in a 5% CO_2 incubator.

After 7 days of differentiation, the NSCs were gently washed three times with PBS for 5 minutes and fixed using 4% tissue cell fixative (Solarbio) at room temperature for 10 minutes. Cells were then washed three times with PBS for 5 minutes and permeabilized using PBS with 0.2% Triton X-100, Amresco, Framingham, MA, USA (PBST) for 10 minutes. After blocking with 5% horse serum in PBST for 30 minutes, the NSCs were incubated with the following primary antibodies: βIII tubulin (a specific marker for neurons, mouse monoclonal, Santa Cruz Biotechnology, Santa Cruz, CA, USA, Cat# sc-80005, 1:400); glial fibrillary acidic protein (GFAP, a specific marker for astrocytes, goat polyclonal, Abcam, Cambridge, UK, Cat# ab53554, 1:500); and ionized calcium-binding adapter molecule 1 (Iba1, a specific marker for microglia, goat polyclonal, Abcam, Cat# ab5076, 1:500). Primary antibodies were incubated at 4°C for 20 hours, and then the cells were washed three times with PBS for 5 minutes, after which the NSCs were incubated with the following secondary antibodies at room temperature for 2 hours: Alexa Fluor 488 labeled anti-mouse IgG (Beyotime, Shanghai, China, A0428, 1:500); rhodamine-labeled anti-rabbit IgG (goat, ZSGB-Bio, Beijing, China, Cat# ZF0316, 1:500); Alexa Fluor 555-labeled anti-

rabbit IgG (Beyotime, Cat# A0453, 1:500). Then the cells were washed three times with PBS for 5 minutes and blocked again using 5% serum for 30 minutes. The NSCs were then incubated with anti-GFP antibody (chicken polyclonal, Abcam, Cat# 13970, 1:500, 0.3% prepared in PBST) at 4°C for 20 hours, followed by Alexa Fluor 488 labeled anti-chicken IgG (Beyotime, Cat# A0428, 1:500) secondary antibody at room temperature for 2 hours. Finally, the nucleus was stained using Hoechst 33258 (Beyotime, Cat# C1011, 1:1000) at room temperature for 5 minutes, and the cells were washed by PBS three times for 5 minutes before observation under the confocal microscope (Nikon, Tokyo, Japan).

Cell transplantation

After *in vitro*, NSCs were infected with lentivirus-GFP for 1 week, the neurospheres were digested with accutase, counted, centrifuged, and resuspended in PBS to prepare a single-cell suspension with a cell density of 1×10^5 cells/μL. The mice (40 weeks old) were anesthetized with 1% sodium pentobarbital solution (Sigma, Cat#57-33-0), and the bilateral hippocampal CA1 region (–2.00 mm anteroposterior, ±1.60 mm mediolateral, –1.75 mm dorsoventral, relative to Bregma) was stereotaxically injected by a 34-gauge metal needle with 2 μL NSCs at 0.2 μL/min. The injecting needle was left in place for 10 minutes after the injection was complete. The mouse scalp was sutured and reinforced with dental cement (Heraeus, Hanau, Germany) to avoid cracking.

Behavioral tests

The animal behavioral tests were performed sequentially starting 4 weeks after NSC transplantation.

T-maze test

The T-maze test was used to examine the spatial working memory abilities of mice (Deacon and Rawlins, 2006). The T-maze (length 35 cm, width 7.5 cm, height 15 cm) consisted of three arms, the main arm and two choice arms. Each arm was equipped with a door that could slide up and down. The experiment consisted of three parts. The first 3 days were the adaptation stage, during which the mice were free to explore the T-maze for 10 minutes. During the training stage, which began on the fourth day, 1–2 mL diluted sweet milk was placed as a reward at the ends of each arm. The mouse was initially placed in the main arm and allowed to freely choose a direction. After the mouse entered an arm, the contralateral door was closed. The mice were then returned to the starting point. During the test stage, the doors were opened to allow the mice to select an arm, and all the arm choices were recorded. A mouse choosing the contralateral side was marked as a correct choice, whereas the ipsilateral side was marked as an error. Each mouse performed 15 trials in succession. The reward was prepared as a 1:1 (v/v) ratio of water/full-fat sweetened condensed milk. The numbers of correct and wrong choices were recorded, and the success rate was calculated for correct choices.

Novelty recognition task

The novelty recognition experiment was performed to test the learning and memory abilities of mice (Bevins and Besheer, 2006). The experiment was composed of three segments. First, during the adaptation stage, which lasted 3 days, the mice were placed in the experimental box (40 cm × 40 cm square box) at the same time each day and allowed to freely explore for 10 minutes. The cabinet was cleaned with 75% ethanol between animals to prevent odors from affecting the following animal. The training stage began on the fourth day. The mice were placed in the experimental box, which contained two identical objects, and were allowed to explore for 5 minutes freely. The time spent exploring the two objects was recorded. During the test stage, the mice were tested after 30 minutes. The mice were placed in the experimental box in which one of the two identical objects was replaced with a novel object and were allowed to freely explore for 5 minutes. The time spent exploring both the familiar and novel objects was recorded.

The delayed matching-to-place task

The delayed matching-to-place task was performed to evaluate the short-term spatial learning and memory abilities of the mice (Nakazawa et al., 2003). The experiment lasted for 7 days, including 3 days of training and 4 days of testing. During the training period, a platform was exposed 1 cm above the water surface and marked with a flag. The mice were placed in the water starting in each quadrant (1–4), sequentially, during each trial and allowed to find the platform within 90 seconds. If the mouse successfully found the platform, it was allowed to remain on the platform for 15 seconds before being returned to its cage. If the mouse failed to find the platform, the mouse was directed to the platform at the end of 90 seconds and allowed to remain on the platform for 15 seconds before being returned to its cage. During the testing phase, the water was turned an opaque white color by the addition of food-grade titanium dioxide, and the platform was placed 1 cm below the water surface with the flag removed. The platform position was different each day and did not appear in the same quadrant for 2 consecutive days. The following procedure was repeated daily: the mice were placed in the water in a different starting quadrant, moving in a clockwise direction. During each trial, the mice were allowed to explore the tank for 90 seconds and allowed to remain on the platform for 15 seconds. If they were unable to locate the platform within 90 seconds, they were directed to the platform and allowed to remain on the platform for 15 seconds. The time at which the mouse reached the platform quadrant for the first time was recorded. Because the platform position changed in each trial, a shorter escape latency indicated a better short-term memory for the mice across the four trials each day.

Morris water maze

The classic Morris water maze test was performed to test the long-term spatial learning and memory abilities of the mice. The experimental procedure was performed as described by Qing et al. (2008). The water maze equipment consisted of a pool 120 cm in diameter and 80 cm in height and a circular platform with a 10-cm diameter. During the experiment, the water temperature was maintained at 22–25°C. The platform was fixed in the first quadrant, and the position of the platform remained unchanged during the entire experimental period. The test lasted for 6 days. The first day was for adaptive training. The platform was exposed above the water surface by 1 cm, a flag was inserted into the platform, and the mice were trained by placing the mice in the water starting in quadrants 2–4, sequentially, until the mice found the platform (in quadrant 1). If the mice failed to find the platform within 90 seconds, they were guided to the platform. The mice were allowed to remain on the platform for 15 seconds before removal. Each mouse was trained in intervals of 60 minutes, starting from a new quadrant in each session. The training was performed from the second to the fifth days. Food-grade titanium dioxide was added to the water to make it an opaque white, the platform was placed 1 cm under the water surface with the flag removed, and the above experimental steps were repeated. On the 6th day, the test was performed with the platform removed, and the platform-finding latency and swimming speed were recorded.

Thioflavin S staining and immunohistochemistry

The mice (n = 6/group after completing behavioral tests 12 weeks after NSC transplantation) were anesthetized with 1% sodium pentobarbital (60 mg/kg, intraperitoneal injection), and the brain was perfused with 0.9% normal saline. The mouse brain samples were isolated and fixed in 4%

paraformaldehyde at 4°C for 24 hours and dehydrated using 20% and 30% sucrose gradients. The brains were then sliced at a thickness of 30 μm. The brain slices were collected in 24-well plates supplemented with antifreeze (containing 30% ethylene glycol and 30% sucrose in PBS) and stored at –20°C until use.

To perform Thioflavin S (ThS) staining, the brain slices were placed in 24-well plates supplemented with PBS and rinsed twice with PBS for 10 minutes to remove the antifreeze. The brain slices were rinsed for 10 minutes with 50% ethanol and then incubated in 1% ThS (dissolved in 80% ethanol, Sigma, Cat# 1326-12-1) for 1 minute. The brain slices were rinsed with 50% ethanol, 20% ethanol, and pure water sequentially, with each rinse step performed three times for 10 minutes each. The brain slices were observed under the confocal microscope.

For immunohistochemistry, brain slices were placed into a 24-well plate, rinsed with PBS three times for 5 minutes each, and permeabilized with PBST at room temperature for 1 hour. The brain slice was then incubated with 5% horse serum in PBST at room temperature for 2 hours to block the heteroprotein binding and reduce background. The brain slices were incubated with the chicken-derived GFP monoclonal primary antibody (chicken polyclonal, Abcam, Cat# ab13970, 1:1000, prepared in 3% horse serum in PBST) at 4°C for 16 hours. The brain slices were then rinsed three times in PBS for 5 minutes each and incubated with a second primary antibody, either neuronal neuron (NeuN, mouse monoclonal, Abcam, Cat# ab104224, 1:400), glial fibrillary acidic protein (GFAP, goat polyclonal, Abcam, Cat# ab53554, 1:500) or Iba1 (goat polyclonal, Abcam, Cat# ab5076, 1:500) at 4°C for 20 hours. Appropriate secondary antibodies were incubated at room temperature for 2 hours. The secondary antibodies were diluted in PBST as follows: donkey anti-goat IgG H&L (Alexa Fluor® 555; Abcam, ab150130, 1:500), donkey anti-rabbit IgG H&L (Alexa Fluor® 555; Abcam, ab150074, 1:500), and donkey anti-chicken IgY H&L (Alexa Fluor® 488; Abcam, ab63507, 1:500). The brain slices were rinsed three times with PBS for 5 minutes. The brain slices were flattened on a glass slide and covered with a coverslip before adding a drop of 4′,6-diamidino-2-phenylindole-containing antifade solution (Solarbio, Cat# S2110). Once the agent was completely diffused, the four corners of the coverslip were fixed with transparent nail polish and allowed to dry. The brain slices were observed under a confocal microscope.

Western blot assay

Mice (*n* = 6/group) that had completed behavioral tests 12 weeks after NSC transplantation were anesthetized with 1% sodium pentobarbital to obtain hippocampal tissues. Hippocampal tissues were homogenized and lysed in radioimmunoprecipitation assay buffer containing phosphatase and protease inhibitors (Roche, Basel, Switzerland). The lysates were analyzed by 10% sodium dodecyl sulfate-polyacrylamide gel electrophoresis and transferred onto a polyvinylidene fluoride (PVDF) membrane. The PVDF membrane was blocked in 2% bovine serum albumin for 2 hours at room temperature and then incubated overnight at 4°C with the following primary antibodies: extracellular regulated protein kinase 1/2 (ERK1/2; rabbit, Cell Signaling, Danvers, MA, USA, Cat# 4695, 1:2000), phosphorylated-ERK1/2 (rabbit, Cell Signaling, Cat# 9101, 1:2000), cyclic adenosine monophosphate-response element-binding protein (CREB; rabbit, Cell Signaling, Cat# 4034, 1:2000), phosphorylated CREB (rabbit, Cell Signaling, Cat# 4095, 1:2000), nuclear factor kappa beta (NFκB; rabbit, Cell Signaling, Cat# 3034, 1:2000), phosphorylated-NFκB (rabbit, Cell Signaling, Cat# 3034, 1:2000), tau (rabbit, 1:1000, Abcam, Cat# ab47579), phosphorylated-paired helical filaments (PHF)-tau pSer202+Thr205 (AT8) (mouse, Thermos Fisher Scientific, Waltham, MA, USA, Cat# MN1020, 1:1000), Ca^{2+}/calmodulin-dependent protein kinase II (CamKII; rabbit, Abcam, Cat# ab134041, 1:1000), and phosphorylated-CamKII (rat, Santa Cruz Biotechnology, Cat# Sc-32289, 1:1000). Membranes were rinsed four times with Tris-buffered saline containing Tween-20 for 10 minutes each time. The PVDF membrane was then incubated with the secondary antibody (horseradish peroxidase-labeled goat anti-mouse IgG, 1:5000) at room temperature for 2 hours. The non-specifically bound secondary antibody was removed by washing five times with Tris-buffered saline containing Tween-20 for 10 minutes each time. The protein bands were visualized using an enhanced chemiluminescence detection system (Bio-Rad, Hercules, CA, USA), and bands were measured and analyzed using ImageJ software (National Institutes of Health, Bethesda, MD, USA).

Proteomics analysis

The proteomic experiment was performed by Shanghai Cuseq Bio-Medical Technology Co. Ltd. (Shanghai, China).

Sample preparation

Brain samples were obtained from mice after completing behavioral tests 12 weeks after NSC transplantation. Brain tissues were lysed in lysis buffer (2% sodium dodecyl sulfate, 7 M urea, 1× protease inhibitor cocktail [Roche, Basel, Switzerland]), ultrasonicated on ice, and centrifuged at 15,000 r/min for 15 minutes at 4°C, the supernatant containing proteins was collected and re-dissolved in 500 mM triethylammonium bicarbonate. Then, 100 μg protein (quantified using the Bradford assay) from each sample was placed into a new tube, and the final volume was adjusted to 100 μL with 8 M urea, followed by the addition of 11 μL 1 M dithiothreitol (Solarbio) and incubation at 37°C for 1 hour. To remove urea, the samples were centrifuged at 15,000 r/min at 4°C three times following the addition of 100 mM triethylammonium bicarbonate and 120 μL 55 mM iodoacetamide was added to the sample and incubated for 20 minutes, protected from light at room temperature. Then proteins were digested with sequence-grade modified trypsin (Promega, Madison, WI, USA).

Data-dependent acquisition: nano-high performance liquid chromatography-mass spectrometry/mass spectrometry analysis

The peptide mixture was analyzed by reversed phase-reversed phase-liquid chromatography-mass spectrometry (MS)/MS for data-dependent acquisition analysis. The peptide mixture was first separated by a reverse-phase column (XBridge C18 column, 4.6 mm × 250 mm, 5 μm, Waters Corporation, Milford, MA, USA) at high pH and then analyzed by an on-line nanospray liquid chromatography-MS/MS on an Orbitrap Fusion Lumos (Thermo Fisher Scientific) coupled to a Nano ACQUITY UPLC system (Waters Corporation). The mass spectrometer was run under data-dependent acquisition mode and automatically switched between MS and MS/MS. The parameters were as follows: (1) MS: scan range (m/z) = 350–1200; resolution = 60,000; automatic gain control target = 400,000; maximum injection time = 50 ms; include charge states = 2–6; Filter Dynamic Exclusion: exclusion duration = 30 seconds; (2) High-energy collision dissociation-MS/MS: resolution = 30,000; automatic gain control target = 500,000; maximum injection time = 64 ms; collision energy = 35%; stepped collision energy = 5%. Raw data obtained during data-dependent acquisition were processed and analyzed by Spectronaut Pulsar 11.0 (Biognosys AG, Schlieren, Switzerland). Pulsar was set up to search the database of the UniProt-mouse, assuming trypsin as the digestion enzyme. Carbamidomethylation (C) was specified as the fixed modification. Oxidation (M) was specified as the variable modifications.

Data-independent acquisition: nano-high performance liquid chromatography-MS/MS analysis

The peptides were re-dissolved in 30 µL solvent C (A: 0.1% formic acid in water) and analyzed by on-line nanospray liquid chromatography-MS/MS on an Orbitrap Fusion Lumos (Thermo Fisher Scientific) coupled to an Easy-nLC 1200 system (Thermo Fisher Scientific). A 10 µL volume of each peptide sample was loaded onto the trap column (Thermo Fisher Scientific, Acclaim PepMap C18, 100 µm × 2 cm), with a flow rate of 300 nL/min and subsequently separated on the analytical column (Acclaim PepMap C18, 75 µm × 15 cm) with a set gradient, from 5% D (D: 0.1% formic acid in ACN) to 8% D in 3 minutes; from 8% D to 22% D between 3 and 82 minutes; from 22% D to 35% D between 82 and 106 minutes; from 35% D to 90% D between 106 and 118 minutes; maintained at 90% D for 5 minutes; from 90% D to 3% D in 0.1 minute; and maintenance of 3% D until 120 minutes. The column flow rate was maintained at 500 nL/min with the column temperature of 40°C. An electrospray voltage of 2.1 kV versus the inlet of the mass spectrometer was used. The mass spectrometer was run under data-dependent acquisition mode and automatically switched between MS and MS/MS mode. The parameters were as follows: (1) MS: scan range (m/z) = 350–1200; resolution = 120,000; automatic gain control target = 500,000; maximum injection time = 60 ms; (2) High-energy collision dissociation-MS/MS: resolution = 50,000; automatic gain control target = 1,000,000; maximum injection time = 100 ms; collision energy = 35%; stepped collision energy = 5%.

Data analysis

Raw data of data from the independent acquisition were processed and analyzed by Spectronaut Pulsar 11.0 (Biognosys AG) using default parameters (BGS Factory Settings (default)). After Student's *t*-test, differentially expressed proteins were filtered according to $P < 0.05$ and Fold-Change > 1.5. Differentially expressed proteins were analyzed by Kyoto Encyclopedia of Genes and Genomes (KEGG) pathway analysis (https://www.genome.jp/kegg/) and Gene Ontology (GO) classification (http://geneontology.org/). The protein interactions were analyzed by STRING software (http://https://string-db.org/).

Statistical analysis

Comparisons between two groups were performed using unpaired, two-tailed Student's *t*-test, and multiple comparisons were performed by one-way analysis of variance followed by Tukey's *post hoc* tests. The data are expressed as the mean ± standard error of the mean (SEM). $P < 0.05$ was considered significant.

Results

Primary NSCs can be differentiated into neurons and astrocytes *in vitro* and *in vivo*

To investigate the differentiation of NSCs, we initially examined the differentiation of primary NSCs *in vitro*. On day 7, the lentivirus carrying the fluorescent GFP plasmid was successfully infected into primary NSCs (**Additional Figure 1A–D**). After transfection, NSCs were aggregated into neurospheres (**Additional Figure 1E–F**). After being cultured under differentiation conditions, the immunochemistry results showed that primary NSCs expressing GFP were stably differentiated. GFP colocalized with both GFAP-marked astrocytes (red) and βIII tubulin-marked neurons (red, **Figure 1**), suggesting that primary NSCs were able to differentiate into both neurons and astrocytes *in vitro*.

We also examined the differentiation of primary NSCs *in vivo*. The results of immunofluorescence staining showed that GFP-marked NSCs colocalized with GFAP-marked astrocytes and NeuN-marked neurons in the brains of Tg-tau mice, suggesting that the transplanted NSCs were able to differentiate into both neurons and astrocytes *in vivo* (**Figure 2**), consistent with the *in vitro* experiment, although at lower levels. Interestingly, the *in vivo* study also showed the colocalization between GFP and Iba1, indicating that the NSCs were also able to differentiate into microglia, which was not observed in the *in vitro* study. Because microglia are functionally associated with inflammation (Gomes et al., 2013), the differentiation of primary NSCs into microglia *in vivo* but not *in vitro* could be due to the presence of inflammation *in vivo* resulting in the differentiation of primary NSCs into microglia.

NSC transplantation improves the short-term memory of the Tg-tau mouse

The above results suggested that transplanted NSCs were able to differentiate into neurons, which triggers us to explore the effects of transplanted NSCs on the learning and memory abilities in AD model mice. The aggregation associated with abnormal tau phosphorylation represents a primary pathological feature of AD. Therefore, we selected a tau transgenic mouse model to serve as a tauopathy model. The Tg-Tau mouse model used in this study shows similar pathological symptoms as AD, including the formation of NFTs, the shrinkage of the brain volume, and a decline in memory abilities (Ramsden et al., 2005). We performed a series of animal behavioral tests to investigate the effects of primary NSC transplantation into the hippocampus on the learning and memory abilities of Tg-Tau mice. We initially examined the spatial working memory of Tg-tau mice, 7 weeks after NSC transplantation, using the T-maze task (**Figure 3A**). As shown in **Figure 3**, the success rates gradually increased from 53.3% to 72.2% from training day 1 to day 10 in the Tg + NSCs group but remained between 40% and 45% in the Tg + PBS group. On day 10, the success rate of the Tg + NSCs group was significantly higher than that of the Tg + PBS group ($P < 0.05$; **Figure 3B** and **C**), suggesting that NSC transplantation greatly improved the spatial working memory of Tg-tau mice.

We further explored the short-term memory of Tg-tau mice by performing the novelty recognition test. Mice in the Tg + NSCs group showed higher curiosity, exploring new objects more than familiar ones ($P < 0.05$) at similar levels as WT mice, whereas the PBS-treated Tg-tau mice spent a much longer time exploring old objects than new ones ($P > 0.05$; **Figure 3D** and **E**), indicating that the short-term memory of Tg-tau mice was significantly increased by NSC transplantation.

The above results indicated that NSC transplantation could improve the short-term memory of AD model mice, which was further confirmed by the short-term water maze test. Mice in the WT and Tg + NSCs groups showed a gradual decrease in the escape latency over time, whereas mice in the Tg + PBS group required significantly longer times to find the platform ($P < 0.001$, *vs*. WT group; **Figure 3F–H**) than the mice in the WT and Tg + NSCs groups. Together, these results indicated that spatial short-term memory was significantly improved by NSC transplantation.

The Morris water maze test was also performed to assess long-term spatial learning and memory in Tg-tau mice 4 weeks after NSC transplantation. As shown in **Additional Figure 2**, during the first 3 days of training, the mice in the Tg + NSCs group had shorter escape latencies than mice in the Tg + PBS group ($P = 0.41$), but the latencies remained longer than those in the WT mice ($P = 0.35$). However, on testing day 5, no significant differences were observed in either the frequency of crossing the platform ($P = 0.17$) or latency ($P = 0.41$) among the three groups, indicating that NSC transplantation did not impact the long-term memories of Tg-tau mice.

NSC transplantation reduces mature NFTs in a Tg-tau mouse

The above data indicated that NSC transplantation could improve the spatial short-term memory of Tg-tau mice; however, the effects of NSC transplantation on the

pathogenesis of Tg-tau mice remained to be determined. Pathological tau aggregation was examined by ThS staining. As shown in **Figure 4**, aggregation was significantly reduced in the CA1 region of the Tg + NSCs group compared with that in the Tg + PBS group ($P < 0.01$). However, no significant changes in either the dentate gyrus or CA3 region were observed between the Tg + NSCs and Tg + PBS groups (both $P > 0.05$; **Figure 4A–F**). The protein expression levels of tau and p-tau were significantly increased in Tg + PBS mice compared with those in WT mice (both $P < 0.001$); however, these levels were decreased in the Tg + NSCs mice (both $P < 0.05$; **Figure 4G–I**). These results suggested that the abnormal tau aggregation observed in the transplantation area was reduced by NSC transplantation.

NSC transplantation leads to significant changes in differentially expressed proteins associated with many biological processes

We applied proteomic techniques to analyze the differential expression of proteins in the hippocampus among WT, Tg + NSCs, and Tg + PBS groups. Triplicate samples were analyzed for each group. A total of 4815 proteins were identified and quantified, including 527 proteins that showed significant changes (fold-change > 1.5, $P < 0.05$) between the Tg + PBS and Tg + NSCs groups. In particular, 239 significantly differentially expressed proteins overlapped between the WT *vs*. Tg + PBS comparison and the Tg + PBS *vs*. Tg + NSCs comparison, including 81 significantly changed proteins that overlapped between the WT *vs*. Tg + NSCs and Tg + PBS *vs*. Tg + NSCs comparisons, and 226 significantly changed proteins that were specifically identified in the Tg + PBS *vs*. Tg + NSCs comparison. Among the 239 significantly changed proteins identified in both the WT *vs*. Tg + PBS group and the Tg + PBS *vs*. Tg + NSCs group comparisons, almost all of the proteins (235 of 239) were restored in the Tg + NSCs group compared with the Tg + PBS group. Furthermore, approximately 105 proteins were found to change consistently in both the WT and Tg + NSCs groups when compared with those in the Tg + PBS group. The findings suggested that the proteins identified in the Tg + PBS *vs*. Tg + NSCs comparison reflected protein expressions altered by NSC treatment in comparison to that by PBS treatment (**Figure 5A**).

We further analyzed 340 significantly changed proteins associated with NSC treatment and found that 78 proteins were upregulated, whereas 262 proteins were downregulated. Through KEGG pathway analysis, these proteins were found to be enriched in long-term potentiation (LTP)-, glutamate synapse-, and dopamine synapse-related pathways (**Figure 5B** and **C**). Interestingly, the proteins associated with LTP were primarily upregulated. Ca^{2+}/calmodulin-dependent kinase II (CaMKII) is an abundant synaptic protein that has been considered to act as a key mediator for LTP (Pi et al., 2010). Thus, we extracted the proteins from the CA1 region of the mouse brain and examined the expression level of CamKII by western blot, which showed that the protein level of CamKII significantly decreased in the Tg + PBS group compared with that in the WT group ($P < 0.001$); however, CaMKII expression was dramatically increased in response to NSC transplantation ($P < 0.001$, *vs*. Tg + PBS group; **Figure 5D**). Because LTP is considered to represent a primary factor in memory ability, these results suggested the NSC transplantation increased the expression of CamKII in the LTP pathway, contributing to the restoration of short-term memory among tau transgenic mice. Other pathways, such as the peroxisome proliferator-activated receptor (PPAR) signaling pathway, the fatty acid metabolic pathway, the cyclic adenosine monophosphate signaling pathway, and the Ca^{2+} signaling pathway, were also associated with proteins enriched by NSC transplantation (**Additional Figure 3**). We also screened several differentially expressed proteins that were associated with tau pathologies, including Fas-associated factor 1 (FAF1), S100A6, S100A4, S100A1, filamin A (FLNA), sequestosome-1 (SQSTM1), CD44, annexin 2 (ANXA2), HTRA1, and heat shock protein family B member 1 (HSPB1). These proteins have been reported to have direct or indirect interactions with the microtubule-associated protein tau (**Figure 5E** and **F**).

Through the analysis of GO classifications, we also found that significantly changed proteins were enriched in neurogenesis, the regulation of synaptic plasticity, neuron development, neuron differentiation, and learning and memory-related neurobiological processes (**Additional Figure 4A–C**). These findings indicated that the induction of neurogenesis was associated with the upregulation of neurogenesis-related pathways, such as the mitogen-activated protein kinase (MAPK)-ERK-CREB pathway (Yang et al., 2019). As shown in **Figure 6**, although the protein level of ERK was reduced in Tg mice, and no difference in total ERK was observed between the Tg + NSCs and Tg + PBS mice, phosphorylated ERK was significantly increased in the Tg + NSCs group ($P = 0.046$) compared with that in Tg + PBS mice (**Figure 6A–C**). Similarly, although CREB was expressed at similar levels among the three groups, phosphorylated CREB was also increased in the Tg + NSCs group compared with that in the Tg + PBS group ($P = 0.032$; **Figure 6D–E**). This result implied that the MAPK-ERK-CREB pathway was activated to induce neurogenesis following NSC transplantation. NFκB is an important factor involved in inflammation, and the inhibition of NFκB phosphorylation can reduce inflammatory effects (Ando et al., 2020). NFκB protein expression was greatly induced in the Tg + PBS group compared with that in WT group ($P = 0.0003$) and was significantly reduced in the Tg + NSCs group ($P = 0.0018$, *vs*. Tg + PBS group). However, the levels of phosphorylated NFκB remained unchanged by NSC treatment compared with PBS (**Figure 6F–G**). This finding was consistent with the proteomic analysis, suggesting that although the differentially expressed proteins were associated with inflammation-related pathways, no significant changes were identified.

Discussion

AD is the most common cause of dementia and has broadly affected the health of older people worldwide. During the last two decades, as reported by the World Alzheimer Report 2018, more than 100 drug discovery attempts were performed to identify potential AD treatment mechanisms; however, only four have been approved, and these four can only alleviate AD symptoms, without curing the disease (Patterson and Alzheimer's Disease International, 2018; Mamun et al., 2020). Therefore, the exploration of effective therapies for AD treatment is extremely urgent and necessary. The potential capacity and advanced techniques associated with stem cells have resulted in stem cell transplantation being viewed as a promising strategy for AD treatment. Our present work focused on examining whether endogenous NSC transplantation in the hippocampal CA1 could alleviate the pathological and behavioral symptoms in a mouse model of tauopathy. To reveal the functional abilities of NSCs, we examined the cell types that NSCs could differentiate into and found that NSCs could differentiate into both neurons and astrocytes *in vivo*, which was consistent with the results obtained by *in vitro* study. Additionally, to investigate the role played by NSC transplantation on the cognitive functions of AD mice, we performed behavioral tests and observed that NSC transplantation could alleviate the impaired short-term memory of Tg-tau mice. We further demonstrated that NSC transplantation could reduce tau aggregation in the hippocampal CA1, where the injection was performed, suggesting that the transplanted NSCs were functionally integrated into the brain and play an important role in alleviating AD pathogenesis. Furthermore, to better understand the molecular changes that occur following NSC transplantation in AD model mice, proteomics studies were

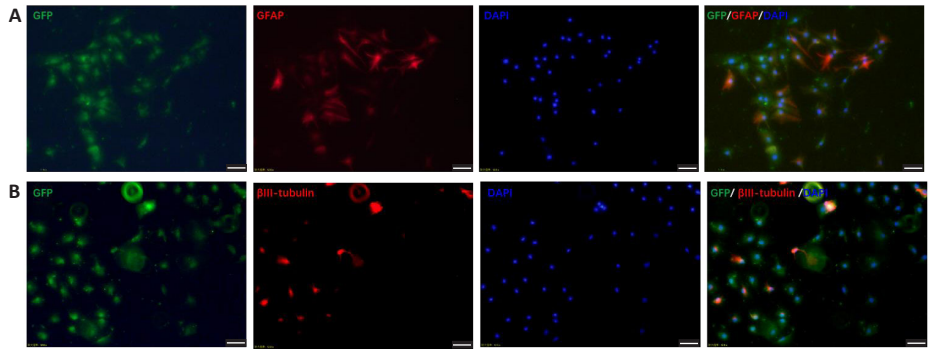

Figure 1 | Primary NSCs differentiate into neurons and astrocytes *in vitro*, 21 days after lentiviral infection.
(A) Primary NSCs differentiated into astrocytes after transfection with lentivirus-GFP. GFAP (red, stained by Alexa Fluor® 555) is a marker for astrocytes. (B) Primary NSCs differentiated into neurons after transfection with lentivirus-GFP (green). βIII tubulin (red, stained by Alexa Fluor® 555) is a marker for neurons. Scale bars: 50 μm. DAPI: 4′,6-Diamidino-2-phenylindole; GFAP: glial fibrillary acidic protein; GFP: green fluorescent protein; NSC: neural stem cell.

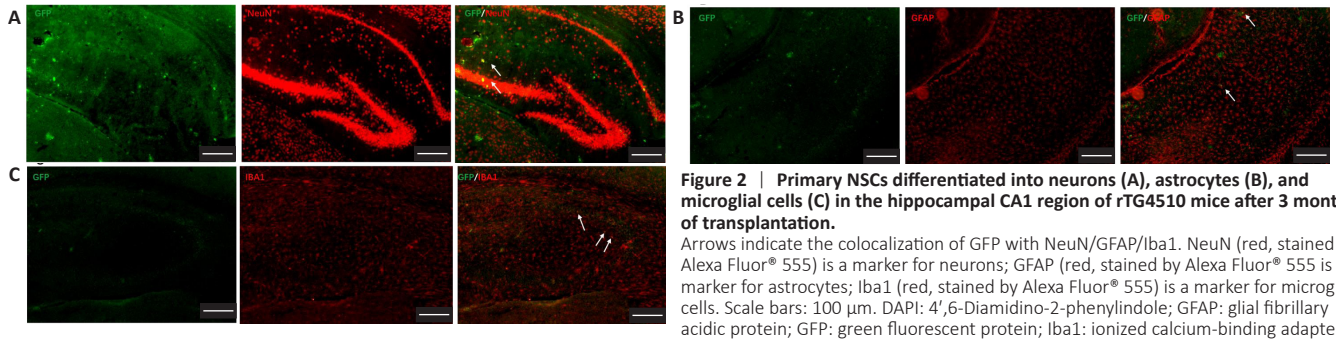

Figure 2 | Primary NSCs differentiated into neurons (A), astrocytes (B), and microglial cells (C) in the hippocampal CA1 region of rTG4510 mice after 3 months of transplantation.
Arrows indicate the colocalization of GFP with NeuN/GFAP/Iba1. NeuN (red, stained by Alexa Fluor® 555) is a marker for neurons; GFAP (red, stained by Alexa Fluor® 555 is a marker for astrocytes; Iba1 (red, stained by Alexa Fluor® 555) is a marker for microglial cells. Scale bars: 100 μm. DAPI: 4′,6-Diamidino-2-phenylindole; GFAP: glial fibrillary acidic protein; GFP: green fluorescent protein; Iba1: ionized calcium-binding adapter molecule 1; NSC: neural stem cell.

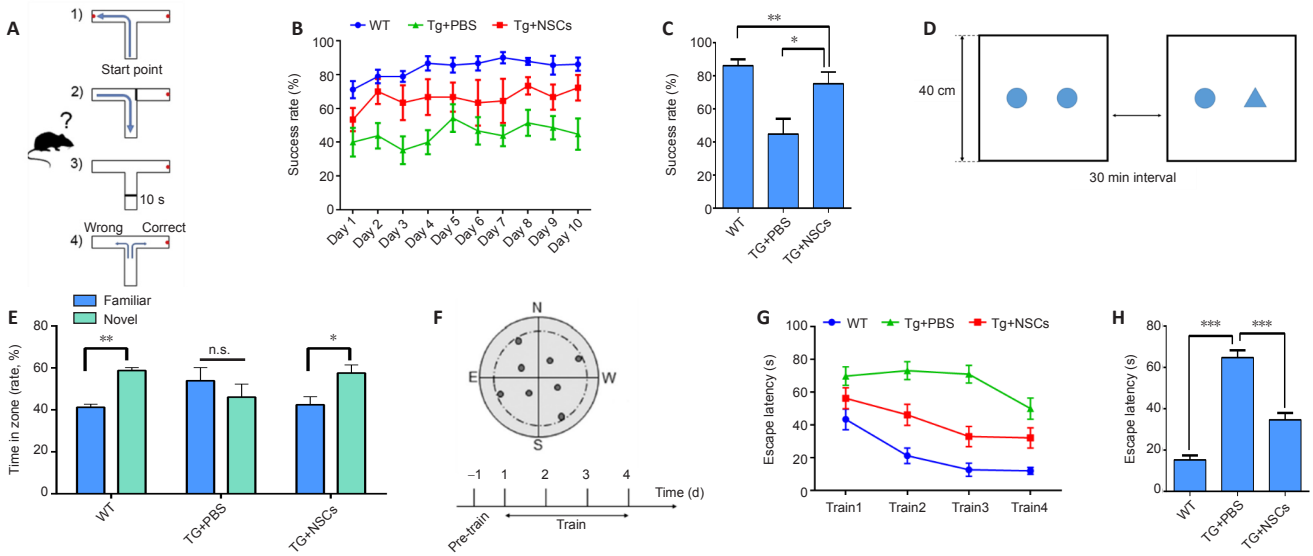

Figure 3 | NSC transplantation ameliorates short-term memory impairment in rTG4510 mice.
(A) Schematic of the T-maze task. (B) The success rate of the T-maze task. (C) The T-maze success rate on day 10. (WT: $n = 6$; Tg + NSCs: $n = 7$; Tg + PBS: $n = 7$). (D) Schematic of the novelty recognition task. (E) Time spent exploring novel and familiar objects (WT: $n = 6$; Tg + NSCs: $n = 10$; Tg + PBS: $n = 8$). (F) Schematic of the delayed matching-to-place task. (G) Escape latency of trials 1–4 in the delayed matching-to-place task. (H) Average escape latency of all trials of the delayed matching-to-place task (WT: $n = 6$; Tg + NSCs: $n = 8$; Tg + PBS: $n = 6$). Data are expressed as the mean ± SEM. $^*P < 0.05$, $^{***}P < 0.001$ (one-way analysis of variance followed by Tukey's *post hoc* test). The experiments were repeated three times. E: East; n.s.: no significance; N: north; NSC: neural stem cell; PBS: phosphate-buffered saline; S: south; Tg: transgenic mice; W: west; WT: wild-type.

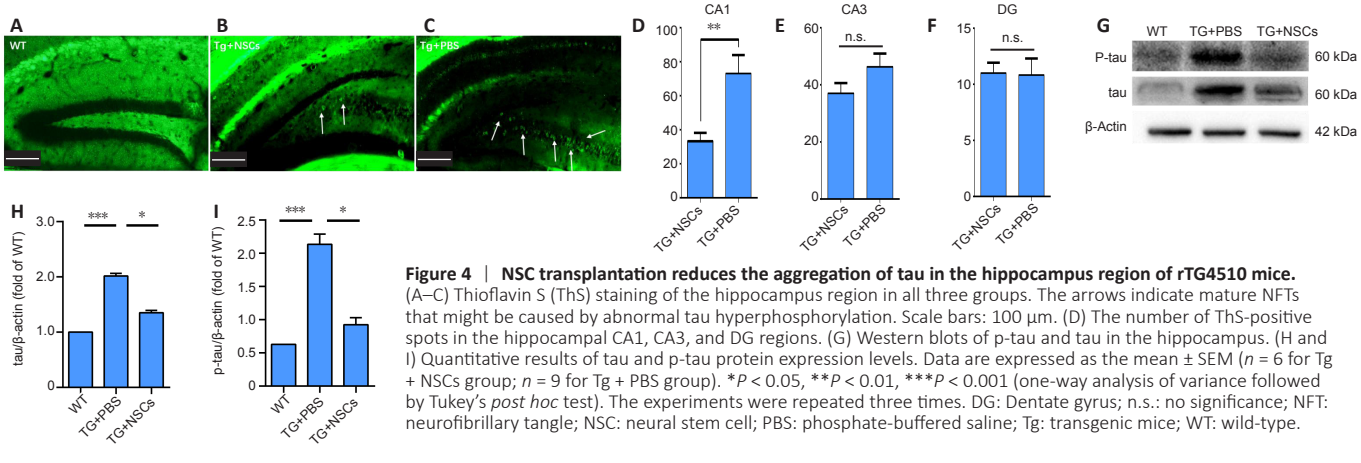

Figure 4 | NSC transplantation reduces the aggregation of tau in the hippocampus region of rTG4510 mice.
(A–C) Thioflavin S (ThS) staining of the hippocampus region in all three groups. The arrows indicate mature NFTs that might be caused by abnormal tau hyperphosphorylation. Scale bars: 100 μm. (D) The number of ThS-positive spots in the hippocampal CA1, CA3, and DG regions. (G) Western blots of p-tau and tau in the hippocampus. (H and I) Quantitative results of tau and p-tau protein expression levels. Data are expressed as the mean ± SEM ($n = 6$ for Tg + NSCs group; $n = 9$ for Tg + PBS group). $^*P < 0.05$, $^{**}P < 0.01$, $^{***}P < 0.001$ (one-way analysis of variance followed by Tukey's *post hoc* test). The experiments were repeated three times. DG: Dentate gyrus; n.s.: no significance; NFT: neurofibrillary tangle; NSC: neural stem cell; PBS: phosphate-buffered saline; Tg: transgenic mice; WT: wild-type.

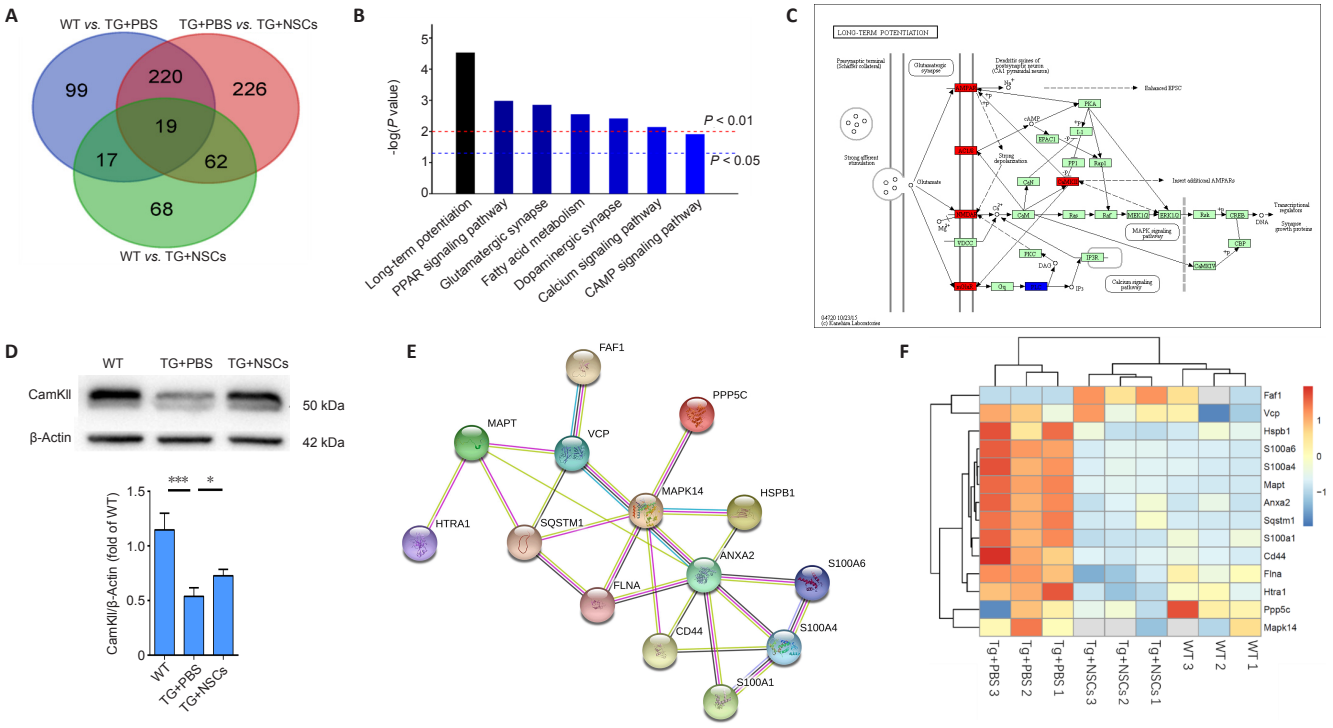

Figure 5 | **Proteomics analysis of NSC transplantation in tau transgenic mice.**
(A) Venn diagram of differentially expressed proteins. (B) Enriched KEGG pathway of proteins with differences in expression levels. (C) Protein expression changes associated with long-term potentiation comparing the Tg + NSCs and Tg + PBS groups. (D) Western blot of CamKII protein expression in the brain. Data are expressed as the mean ± SEM. *P < 0.05, ***P < 0.001 (one-way analysis of variance followed by Tukey's *post hoc* test). (E) Stimulated protein interactions with tau. Network nodes represent proteins that can interact with tau. Edges represent protein-protein associations. Light blue and pink lines represent known interactions; green, red, and blue lines represent predicted protein interactions; light green, black, and light purple lines represent others. (F) Unbiased hierarchical clustering analysis of gene expression changes in the WT, Tg + NSCs, and Tg + PBS groups (n = 3 samples/group). The experiments were repeated three times. KEGG: Kyoto Encyclopedia of Genes and Genomes; NSC: neural stem cell; PBS: phosphate-buffered saline; Tg: transgenic mice; WT: wild-type.

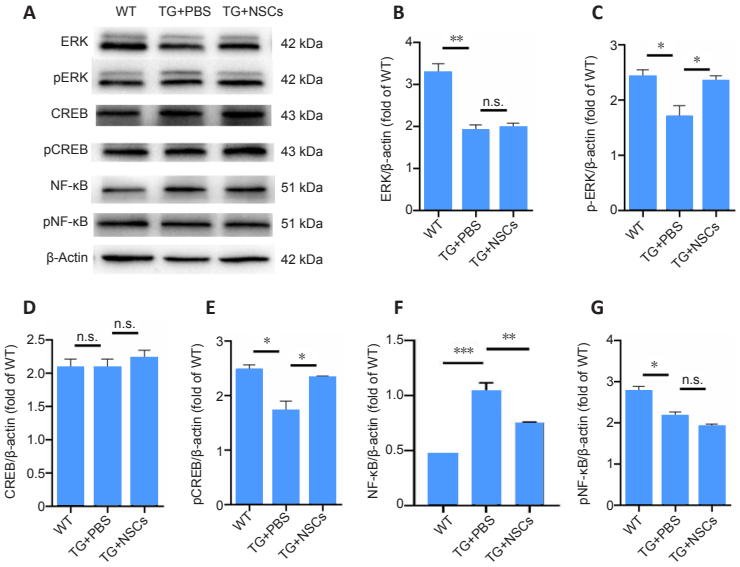

Figure 6 | **Effects of NSC transplantation on ERK, CREB, and NFκB protein expression levels in the hippocampus of rTG4510 mice.**
(A) Western blot bands of ERK, pERK, CREB, p-CREB, NFκB, and pNFκB. (B–G) Quantitative results of ERK, pERK, CREB, p-CREB, NFκB, and pNFκB expression. The target protein expression was normalized against the expression of β-actin. Data are expressed as the mean ± SEM (n = 3/group). *P < 0.05, **P < 0.01 (one-way analysis of variance, followed by Tukey's *post hoc* test). The experiments were repeated three times. CREB: Cyclic adenosine monophosphate-response element-binding protein; ERK: extracellular regulated protein kinase; NFκB: nuclear factor kappa beta; ns: no significance; p-CREB: phosphorylated CREB; PBS: phosphate-buffered saline; pERK: phosphorylated ERK; pNFκB: phosphorylated NFκB; Tg: transgenic mice; WT: wild-type.

performed, which demonstrated that NSC transplantation significantly changed protein expressions patterns associated with many pathways, including LTP, neurogenesis, the regulation of synaptic plasticity, neuron development, neuron differentiation, and learning and memory-related neurobiological processes. The expression changes of key factors involved in LTP and neurogenesis were further verified by western blot analysis. Additionally, a group of proteins functionally related to tau aggregation or misfolding was found to exhibit similar expressional levels between the Tg + NSCs and WT groups, which was consistent with the above results. These multiple cellular, metabolic, and neurobiological changes induced by NSC transplantation indicated that NCS could be comprehensively involved in brain functions and potentially play a role in AD treatment.

Stem cell therapy emerged in the early 2000s and has been explored as a potential treatment for various diseases, especially neurological diseases. Many studies have investigated the application of various types of stem cells, including embryonic stem cells (ESCs), brain-derived NSCs, mesenchymal stem cells, and induced pluripotent stem cells (iPSCs). ESCs, which originate from the blastocyst, have pluripotent characteristics and their applications have been reported for the treatment of brain injuries (Acharya et al., 2009). However, the engraftment of undifferentiated ESCs has disadvantages, including uncontrolled cell growth and high risks of tumor formation (Fong et al., 2010; Duncan and Valenzuela, 2017). Liu et al. (2013) managed to differentiate human ESCs into a nearly uniform population of medial ganglionic eminence-like cells, the transplantation of which

could improve the learning and memory deficits in a murine brain injury model. However, ESC transplantation continues to face ethical and immunogenic issues that must be resolved before they can be used in clinical applications (Duru et al., 2018). Mesenchymal stem cells are another frequently studied stem cell type. Many studies have reported their remarkable properties on neuroprotective paracrine effects, the rescue of cell death, the induction of hippocampal neurogenesis, and the improvement of neuropathology and cognitive functions in many AD models (Zilka et al., 2011; Lee et al., 2012; Yang et al., 2013; Yun et al., 2013; Oh et al., 2015). However, the application of mesenchymal stem cells might be limited due to their low rates of neuronal differentiation and a preference for glial formation *in vivo* (Lee et al., 2003; Duncan and Valenzuela, 2017). Studies of iPSCs have recently established that they are capable of producing autologous pluripotent stem cells, which may represent an effective method for avoiding both ethical and immune rejection issues associated with the use of non-patient-specific sources (Duncan and Valenzuela, 2017). iPSC-derived neurons isolated from AD patients showed pathological disease phenotypes, such as increased cytotoxicity, apoptosis, and neurite length, and increased inflammatory stress factors, indicating that these cells may not be useful for neuroreplacement studies (Balez et al., 2016; Duru et al., 2018).

NSCs are multipotent and are capable of differentiating into central nerve cell types, including neurons and glial cells, indicating the potential for therapeutic applications for many neurodegenerative diseases (Gonzalez et al., 2016). Some cases describing the xenografting of human-derived NSCs into AD rodent models have been described to reduce AD neuropathology, attenuate neuroinflammation, stimulate neurogenesis and synaptogenesis, and restore the cognitive functions in AD model mice (Blurton-Jones et al., 2009; Ager et al., 2015; Li et al., 2016; McGinley et al., 2018). Furthermore, NSC homografts, derived from the adult mouse brain or ESCs, were able to generate cholinergic neurons and increase synaptic strength and memory performance in AD rodent models (Blurton-Jones et al., 2009; Moghadam et al., 2009). Transplanted NSCs have been speculated to be able to differentiate into functional neurons, restoring impaired neural circuitry and cognitive abilities. As predicted, our study demonstrated that NSC grafts could relieve tau pathology and restore spatial short-term memory in Tg-tau mice, which was consistent with the findings of other studies, confirming the great potential and capacity of NSCs in AD treatment. However, transplanted NSCs differentiated into both neurons and astrocytes, which might change the microenvironment in the brain and cause urgent inflammation. Alternatively, a more efficient method may involve the induction of NSC differentiation into specific neuronal cell types *in vitro*, followed by the transplantation of specific neurons into AD model mice for treatment. The microenvironment is also quite important for the proper function of neurons. A recent study (Gantner et al., 2020) reported that differences in the delivery styles of glial cell line-derived neurotrophic factors could cause different graft outcomes. Early glial cell line-derived neurotrophic factor delivery induces the survival and plasticity of non-dopaminergic neurons, leading to motor recovery in PD rats, whereas the delayed exposure to glial cell line-derived neurotrophic factor increased functional recovery via the induction of dopaminergic neuron specification, plasticity, and metabolism (Gantner et al., 2020). Therefore, future work should also focus on identifying better mechanisms for the delivery of specific neurotrophic factors, in addition to NSC grafts, to improve AD treatment.

Systemic studies examining NSC transplantation have not yet been reported. Our work included a proteomics analysis to explore the changes associated with NSC transplantation in a mouse model of tauopathy. Our proteomics study identified and quantified nearly 5000 proteins in total, including 527 proteins with significant changes, which were further analyzed. The data showed that 235 proteins were restored by NSC transplantation compared with the vehicle (PBS) injection. Using the KEGG signaling pathway and GO analyses, significantly changed proteins are found to be enriched in neuronal differentiation, neurogenesis, LTP, synaptic plasticity, and learning and memory-related pathways. These results suggested that the effects of NSC transplantation on memory improvements in AD model mice could be mediated by the differentiation of NSCs and the integration of NSCs into neural circuits, which could alleviate neural circuits impaired by neuronal loss. We also analyzed an additional 187 significantly changed proteins using GO analysis and revealed that they were primarily associated with biosynthetic processes (e.g., organonitrogen, NADP, and nucleotides), which may result in NSC growth and differentiation *in vivo*. No proteins were associated with side effects in tauopathy model mice that were likely to be caused by NSC transplantation, suggesting the safety of endogenous NSC transplantation for AD treatment.

Meanwhile, the proteomic data also revealed several proteins that have been reported to be relevant to tau pathologies. FAF1 is responsible for the cleavage and activation of caspase-3, resulting in the aggregation of hyperphosphorylated tau and NFT formation, initiating the apoptosis of basal forebrain cholinergic neurons in P301L transgenic mice (Kim et al., 2015). HSPB1 has been found to be related to the function of indole/indolylquinoline compounds, which reduce tau misfolding (Chang et al., 2017). HTRA1 belongs to the high-temperature-requirement A family of serine proteases that can degrade aggregated and fibrillary tau, and HTRA1 mRNA levels and activity correlate with elevated tau concentrations (Tennstaedt et al., 2012). S100A1 and S100A6 belong to the same protein family and can bind and regulate the enzymatic activity of serine//threonine protein phosphatase 5C. S100A6 can dephosphorylate tau T231 via PPP5C activation, and S100A1 functions similarly, with overexpression able to induce tau dephosphorylation (Yamaguchi et al., 2012; Haldar et al., 2020). SQSTM1 acts as an autophagy cargo receptor that selectively targets and predominantly cleaves insoluble rather than soluble misfolded tau to alleviate NFT pathology and spreading (Xu et al., 2019). Another study reported that SQSTM1 could prevent tau-seeded aggregation by monitoring endomembrane integrity and reducing the entry of tau seeds into the cytosol (Falcon et al., 2018). Furthermore, CD44 secreted from glioblastoma can induce tau phosphorylation and aggregation, triggering neuron degeneration in the brain (Lim et al., 2018). ANXA2 encodes the Ca^{2+}-regulated plasma membrane-binding protein annexin A2, and its core domain can interact with tau via tau's extreme N-terminus, which is encoded by the first exon (E1). This E1-mediated interaction is responsible for the axonal enrichment of tau and contributes to the redistribution of tau under pathological conditions (Gauthier-Kemper et al., 2018). Most of these proteins function as proteases or proteasomal regulators, and their functions are tightly correlated with tau de/phosphorylation or degradation. All these data suggested that NSC transplantation could regulate the expression of proteases or protein-quality control proteins that play key roles in the degradation of misfolded or insoluble tau proteins and the reduction of tau phosphorylation, alleviating NFT pathology.

Additional details remain to be explored based on the proteomics analysis, which should be explored in future work. For example, significantly changed proteins were also enriched in the PPAR signaling pathway and the fatty acid metabolic pathway. PPAR regulates cell growth and differentiation via the modulation of lipid metabolism, which might play an important role in NSC differentiation *in vivo*.

In the dopamine synapse-related pathway, significantly changed proteins were abundant in post-synaptic neurons, suggesting that the neurons that differentiate from NSCs might connect to upstream dopamine neurons and form synapses, enhancing the signal transmission between neurons, mediated by the cyclic adenosine monophosphate and Ca^{2+} signaling pathways. Furthermore, the roles played by NSC-differentiated cell types, including astrocytes and microglia, can be further studied relative to their relations with inflammation and synaptic plasticity. The current study had limitations. First, the techniques that were used to trace the fates of NSC transplantations, such as the efficiencies of lentiviral GFP transfection and antibody labeling, were still not intuitive. Second, whether the implanted and differentiated neurons successfully integrate into existing neural circuits was not examined by direct experiments. Owing to limitations associated with the available behavioral tests, declining motor abilities in aged mice might introduce bias during tests dependent on motor abilities, such as the Morris water maze, which could disrupt the ability to identify significant impacts. Our future work might focus on revealing the mechanisms through which newly differentiated neurons integrate into neural circuits.

Acknowledgments: *We thank the Biological and Medical Engineering Core Facilities of Beijing Institute of Technology for supporting experimental equipment. We also thank Xuanwu Hospital in Beijing, China for providing the transgenic tau mice.*
Author contributions: *Study design and manuscript drafting: HQ, ZZQ; experiment implementation: HAZ, CXY, KFL, QFY, HL; data analysis: QHY, DS, JZ, ZZQ. All authors read and approved the final manuscript.*
Conflicts of interest: *The authors declare that they have no conflict of interest.*
Financial support: *This work was supported by the National Key Research and Development Program of China, Nos. 2017YFE0117000 (to ZZQ), 2018YFC1312302-3 (to HQ); the Beijing Advanced Innovation Center for Intelligent Robots and Systems of China, No. 2018IRS12 (to ZZQ); and the National Natural Science Foundation of China, Nos. 82001167 (to HL), 81870844 (to HQ), 81701260 (to ZZQ). The funding sources had no role in study conception and design, data analysis or interpretation, paper writing or deciding to submit this paper for publication.*
Institutional review board statement: *The study was approved by the Beijing Animal Ethics Association and Ethics Committee of Beijing Institute of Technology (approval No. SYXK-BIT-school of life science-2017-M03) in 2017.*

Data sharing statement: *Datasets analyzed during the current study are available from the corresponding author on reasonable request.*
Plagiarism check: *Checked twice by iThenticate.*
Peer review: *Externally peer reviewed.*

Open peer reviewer: *Alain Buisson, Université Joseph-Fourier, France.*
Additional files:
Additional Figure 1: *Characterization of NSCs from mouse brain.*
Additional Figure 2: *NSC transplantation does not affect the escape latency in 3 days (A), and frequency (B) and velocity in 5 days (C) during the classic Morris water maze test.*
Additional Figure 3: *Protein expression changes in PPAR signaling pathway (A), calcium signaling pathway (B) and glutamate synapse (C) between Tg + NSCs and Tg + PBS groups.*
Additional Figure 4: *Gene Ontology (GO) classifications of changed proteins with significance in certain pathways, including protein dimerization activity (A), neurogenesis (B), and biosynthetic process (C) between Tg + NSCs and Tg + PBS groups.*
Additional file 1: *Open peer review report 1.*

References

Acharya MM, Christie LA, Lan ML, Donovan PJ, Cotman CW, Fike JR, Limoli CL (2009) Rescue of radiation-induced cognitive impairment through cranial transplantation of human embryonic stem cells. Proc Natl Acad Sci U S A 106:19150-19155.

Ager RR, Davis JL, Agazaryan A, Benavente F, Poon WW, LaFerla FM, Blurton-Jones M (2015) Human neural stem cells improve cognition and promote synaptic growth in two complementary transgenic models of Alzheimer's disease and neuronal loss. Hippocampus 25:813-826.

Ando Y, Keino H, Kudo A, Hirakata A, Okada AA, Umezawa K (2020) Anti-Inflammatory Effect of Dehydroxymethylepoxyquinomicin, a Nuclear factor-κB Inhibitor, on Endotoxin-Induced Uveitis in Rats In vivo and In vitro. Ocul Immunol Inflamm 28:240-248.

Balez R, Steiner N, Engel M, Muñoz SS, Lum JS, Wu Y, Wang D, Vallotton P, Sachdev P, O'Connor M, Sidhu K, Münch G, Ooi L (2016) Neuroprotective effects of apigenin against inflammation, neuronal excitability and apoptosis in an induced pluripotent stem cell model of Alzheimer's disease. Sci Rep 6:31450.

Bernstock JD, Peruzzotti-Jametti L, Ye D, Gessler FA, Maric D, Vicario N, Lee YJ, Pluchino S, Hallenbeck JM (2017) Neural stem cell transplantation in ischemic stroke: A role for preconditioning and cellular engineering. J Cereb Blood Flow Metab 37:2314-2319.

Bevins RA, Besheer J (2006) Object recognition in rats and mice: a one-trial non-matching-to-sample learning task to study 'recognition memory'. Nat Protoc 1:1306-1311.

Blurton-Jones M, Kitazawa M, Martinez-Coria H, Castello NA, Müller FJ, Loring JF, Yamasaki TR, Poon WW, Green KN, LaFerla FM (2009) Neural stem cells improve cognition via BDNF in a transgenic model of Alzheimer disease. Proc Natl Acad Sci U S A 106:13594-13599.

Chang KH, Lin CH, Chen HC, Huang HY, Chen SL, Lin TH, Ramesh C, Huang CC, Fung HC, Wu YR, Huang HJ, Lee-Chen GJ, Hsieh-Li HM, Yao CF (2017) The potential of indole/indolylquinoline compounds in tau misfolding reduction by enhancement of HSPB1. CNS Neurosci Ther 23:45-56.

Cosacak MI, Bhattarai P, Kizil C (2020) Alzheimer's disease, neural stem cells and neurogenesis: cellular phase at single-cell level. Neural Regen Res 15:824-827.

Deacon RM, Rawlins JN (2006) T-maze alternation in the rodent. Nat Protoc 1:7-12.

Duncan T, Valenzuela M (2017) Alzheimer's disease, dementia, and stem cell therapy. Stem Cell Res Ther 8:111.

Duru LN, Quan Z, Qazi TJ, Qing H (2018) Stem cells technology: a powerful tool behind new brain treatments. Drug Deliv Transl Res 8:1564-1591.

Falcon B, Noad J, McMahon H, Randow F, Goedert M (2018) Galectin-8-mediated selective autophagy protects against seeded tau aggregation. J Biol Chem 293:2438-2451.

Fong CY, Gauthaman K, Bongso A (2010) Teratomas from pluripotent stem cells: a clinical hurdle. J Cell Biochem 111:769-781.

Gantner CW, de Luzy IR, Kauhausen JA, Moriarty N, Niclis JC, Bye CR, Penna V, Hunt CPJ, Ermine CM, Pouton CW, Kirik D, Thompson LH, Parish CL (2020) Viral delivery of GDNF promotes functional integration of human stem cell grafts in Parkinson's disease. Cell Stem Cell 26:511-526.e5.

Gauthier-Kemper A, Suárez Alonso M, Sündermann F, Niewidok B, Fernandez MP, Bakota L, Heinisch JJ, Brandt R (2018) Annexins A2 and A6 interact with the extreme N terminus of tau and thereby contribute to tau's axonal localization. J Biol Chem 293:8065-8076.

Gomes C, Ferreira R, George J, Sanches R, Rodrigues DI, Gonçalves N, Cunha RA (2013) Activation of microglial cells triggers a release of brain-derived neurotrophic factor (BDNF) inducing their proliferation in an adenosine A2A receptor-dependent manner: A2A receptor blockade prevents BDNF release and proliferation of microglia. J Neuroinflammation 10:16.

Gonzalez R, Hamblin MH, Lee JP (2016) Neural stem cell transplantation and CNS diseases. CNS Neurol Disord Drug Targets 15:881-886.

Haldar B, Hamilton CL, Solodushko V, Abney KA, Alexeyev M, Honkanen RE, Scammell JG, Cioffi DL (2020) S100A6 is a positive regulator of PPP5C-FKBP51-dependent regulation of endothelial calcium signaling. FASEB J 34:3179-3196.

Kang JM, Yeon BK, Cho SJ, Suh YH (2016) Stem cell therapy for Alzheimer's disease: a review of recent clinical trials. J Alzheimers Dis 54:879-889.

Kim JM, Kim SS, Lee YD (2015) Fas-associated factor 1 promotes in neurofibrillary tangle-mediated cell death of basal forebrain cholinergic neurons in P301L transgenic mice. Neuroreport 26:767-772.

Ji HY, Gu J, Xie LH, Wu XT (2020) Application of stem cells, tissue engineering scaffolds and neurotrophic factors in the treatment of spinal cord injury. Zhongguo Zuzhi Gongcheng Yanjiu 24:4088-4093.

Lee HJ, Lee JK, Lee H, Carter JE, Chang JW, Oh W, Yang YS, Suh JG, Lee BH, Jin HK, Bae JS (2012) Human umbilical cord blood-derived mesenchymal stem cells improve neuropathology and cognitive impairment in an Alzheimer's disease mouse model through modulation of neuroinflammation. Neurobiol Aging 33:588-602.

Lee J, Kuroda S, Shichinohe H, Ikeda J, Seki T, Hida K, Tada M, Sawada K, Iwasaki Y (2003) Migration and differentiation of nuclear fluorescence-labeled bone marrow stromal cells after transplantation into cerebral infarct and spinal cord injury in mice. Neuropathology 23:169-180.

Li M, Guo K, Ikehara S (2014) Stem cell treatment for Alzheimer's disease. Int J Mol Sci 15:19226-19238.

Li X, Zhu H, Sun X, Zuo F, Lei J, Wang Z, Bao X, Wang R (2016) Human neural stem cell transplantation rescues cognitive defects in APP/PS1 model of Alzheimer's disease by enhancing neuronal connectivity and metabolic activity. Front Aging Neurosci 8:282.

Lim S, Kim D, Ju S, Shin S, Cho IJ, Park SH, Grailhe R, Lee C, Kim YK (2018) Glioblastoma-secreted soluble CD44 activates tau pathology in the brain. Exp Mol Med 50:5.

Liu Y, Weick JP, Liu H, Krencik R, Zhang X, Ma L, Zhou GM, Ayala M, Zhang SC (2013) Medial ganglionic eminence-like cells derived from human embryonic stem cells correct learning and memory deficits. Nat Biotechnol 31:440-447.

Mamun AA, Uddin MS, Mathew B, Ashraf GM (2020) Toxic tau: structural origins of tau aggregation in Alzheimer's disease. Neural Regen Res 15:1417-1420.

McGinley LM, Kashlan ON, Bruno ES, Chen KS, Hayes JM, Kashlan SR, Raykin J, Johe K, Murphy GG, Feldman EL (2018) Human neural stem cell transplantation improves cognition in a murine model of Alzheimer's disease. Sci Rep 8:14776.

Moghadam FH, Alaie H, Karbalaie K, Tanhaei S, Nasr Esfahani MH, Baharvand H (2009) Transplantation of primed or unprimed mouse embryonic stem cell-derived neural precursor cells improves cognitive function in Alzheimerian rats. Differentiation 78:59-68.

Nakazawa K, Sun LD, Quirk MC, Rondi-Reig L, Wilson MA, Tonegawa S (2003) Hippocampal CA3 NMDA receptors are crucial for memory acquisition of one-time experience. Neuron 38:305-315.

Oh SH, Kim HN, Park HJ, Shin JY, Lee PH (2015) Mesenchymal stem cells increase hippocampal neurogenesis and neuronal differentiation by enhancing the Wnt signaling pathway in an Alzheimer's disease model. Cell Transplant 24:1097-1109.

Pang ZP, Yang N, Vierbuchen T, Ostermeier A, Fuentes DR, Yang TQ, Citri A, Sebastiano V, Marro S, Sudhof TC, Wernig M (2011) Induction of human neuronal cells by defined transcription factors. Nature 476:220-223.

Patterson C, Alzheimer's Disease International (2018) World Alzheimer report 2018. https://apo.org.au/node/260056: Alzheimer's Disease International. Assessed July 1, 2020.

Pi HJ, Otmakhov N, Lemelin D, De Koninck P, Lisman J (2010) Autonomous CaMKII can promote either long-term potentiation or long-term depression, depending on the state of T305/T306 phosphorylation. J Neurosci 30:8704-8709.

Qing H, He G, Ly PT, Fox CJ, Staufenbiel M, Cai F, Zhang Z, Wei S, Sun X, Chen CH, Zhou W, Wang K, Song W (2008) Valproic acid inhibits Abeta production, neuritic plaque formation, and behavioral deficits in Alzheimer's disease mouse models. J Exp Med 205:2781-2789.

Ramsden M, Kotilinek L, Forster C, Paulson J, McGowan E, SantaCruz K, Guimaraes A, Yue M, Lewis J, Carlson G, Hutton M, Ashe KH (2005) Age-dependent neurofibrillary tangle formation, neuron loss, and memory impairment in a mouse model of human tauopathy (P301L). J Neurosci 25:10637-10647.

Song D, Yang Q, Lang Y, Wen Z, Xie Z, Zheng D, Yan T, Deng Y, Nakanishi H, Quan Z, Qing H (2018) Manipulation of hippocampal CA3 firing via luminopsins modulates spatial and episodic short-term memory, especially working memory, but not long-term memory. Neurobiol Learn Mem 155:435-445.

Tennstaedt A, Pöpsel S, Truebestein L, Hauske P, Brockmann A, Schmidt N, Irle I, Sacca B, Niemeyer CM, Brandt R, Ksiezak-Reding H, Tirniceriu AL, Egensperger R, Baldi A, Dehmelt L, Kaiser M, Huber R, Clausen T, Ehrmann M (2012) Human high temperature requirement serine protease A1 (HTRA1) degrades tau protein aggregates. J Biol Chem 287:20931-20941.

Xu Y, Zhang S, Zheng H (2019) The cargo receptor SQSTM1 ameliorates neurofibrillary tangle pathology and spreading through selective targeting of pathological MAPT (microtubule associated protein tau). Autophagy 15:583-598.

Yamaguchi F, Umeda Y, Shimamoto S, Tsuchiya M, Tokumitsu H, Tokuda M, Kobayashi R (2012) S100 proteins modulate protein phosphatase 5 function: a link between Ca^{2+} signal transduction and protein dephosphorylation. J Biol Chem 287:13787-13798.

Yang H, Xie Z, Wei L, Yang H, Yang S, Zhu Z, Wang P, Zhao C, Bi J (2013) Human umbilical cord mesenchymal stem cell-derived neuron-like cells rescue memory deficits and reduce amyloid-beta deposition in an AβPP/PS1 transgenic mouse model. Stem Cell Res Ther 4:76.

Yang L, Ran Y, Quan Z, Wang R, Yang Q, Jia Q, Zhang H, Li Y, Peng Y, Liang J, Wang H, Nakanishi H, Deng Y, Qing H (2019) Pterostilbene, an active component of the dragon's blood extract, acts as an antidepressant in adult rats. Psychopharmacology (Berl) 236:1323-1333.

Yousefifard M, Rahimi-Movaghar V, Nasirinezhad F, Baikpour M, Safari S, Saadat S, Moghadas Jafari A, Asady H, Razavi Tousi SM, Hosseini M (2016) Neural stem/progenitor cell transplantation for spinal cord injury treatment; A systematic review and meta-analysis. Neuroscience 322:377-397.

Yun HM, Kim HS, Park KR, Shin JM, Kang AR, il Lee K, Song S, Kim YB, Han SB, Chung HM, Hong JT (2013) Placenta-derived mesenchymal stem cells improve memory dysfunction in an Aβ1-42-infused mouse model of Alzheimer's disease. Cell Death Dis 4:e958.

Zilka N, Zilkova M, Kazmerova Z, Sarissky M, Cigankova V, Novak M (2011) Mesenchymal stem cells rescue the Alzheimer's disease cell model from cell death induced by misfolded truncated tau. Neuroscience 193:330-337.

P-Reviewer: Buisson A; C-Editor: Zhao M; S-Editors: Yu J, Li CH; L-Editors: Giles L, Yu J, Song LP; T-Editor: Jia Y

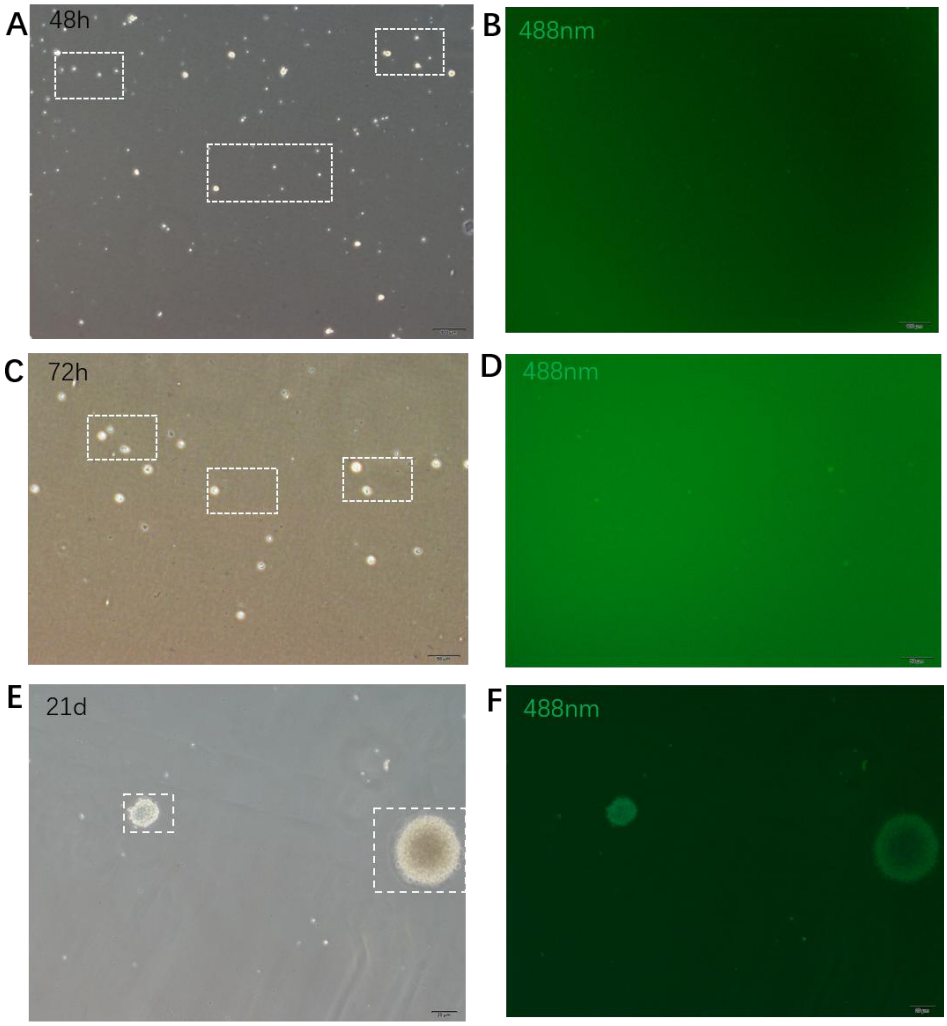

Additional Figure 1 Characterization of NSCs from mouse brain.

(A, C, E) The microscopy view of NSCs at 48 hours (A), 72 hours (C) and 21 days (E) after transfection. (B, D, F) The GFP lentivirus infected NSCs at 48 hours (B), 72 hours (D) and 21 days (F) after transfection. At 21 days, the NSCs were formed neurospheres. The GFP lentivirus infected NSCs can be observed under 488 nm. Scale bars: 100 μm in A, B; 50 μm in C, D; 20 μm in E, F. GFP: Green fluorescent protein; NSCs: neural stem cells. The experiments were repeated by three times.

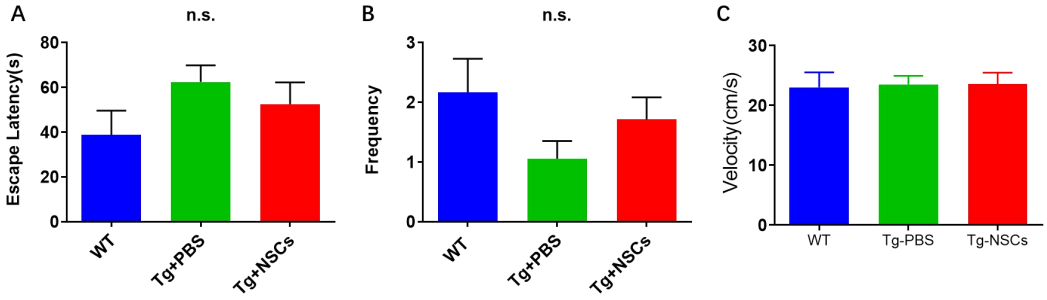

Additional Figure 2 NSC transplantation does not affect the escape latency in 3 days (A), and frequency (B) and velocity in 5 days (C) during the classic Morris water maze test.

Data are expressed as mean ± SEM (WT: $n = 6$; Tg + NSCs: $n = 8$; Tg + PBS: $n = 6$), and were analyzed by one-way analysis of variance followed by Tukey's post hoc test. The experiments were repeated by three times. n.s.: No significance; NSC: neural stem cells; PBS: phosphate buffered saline; Tg: transgenic mice; WT: wild-type.

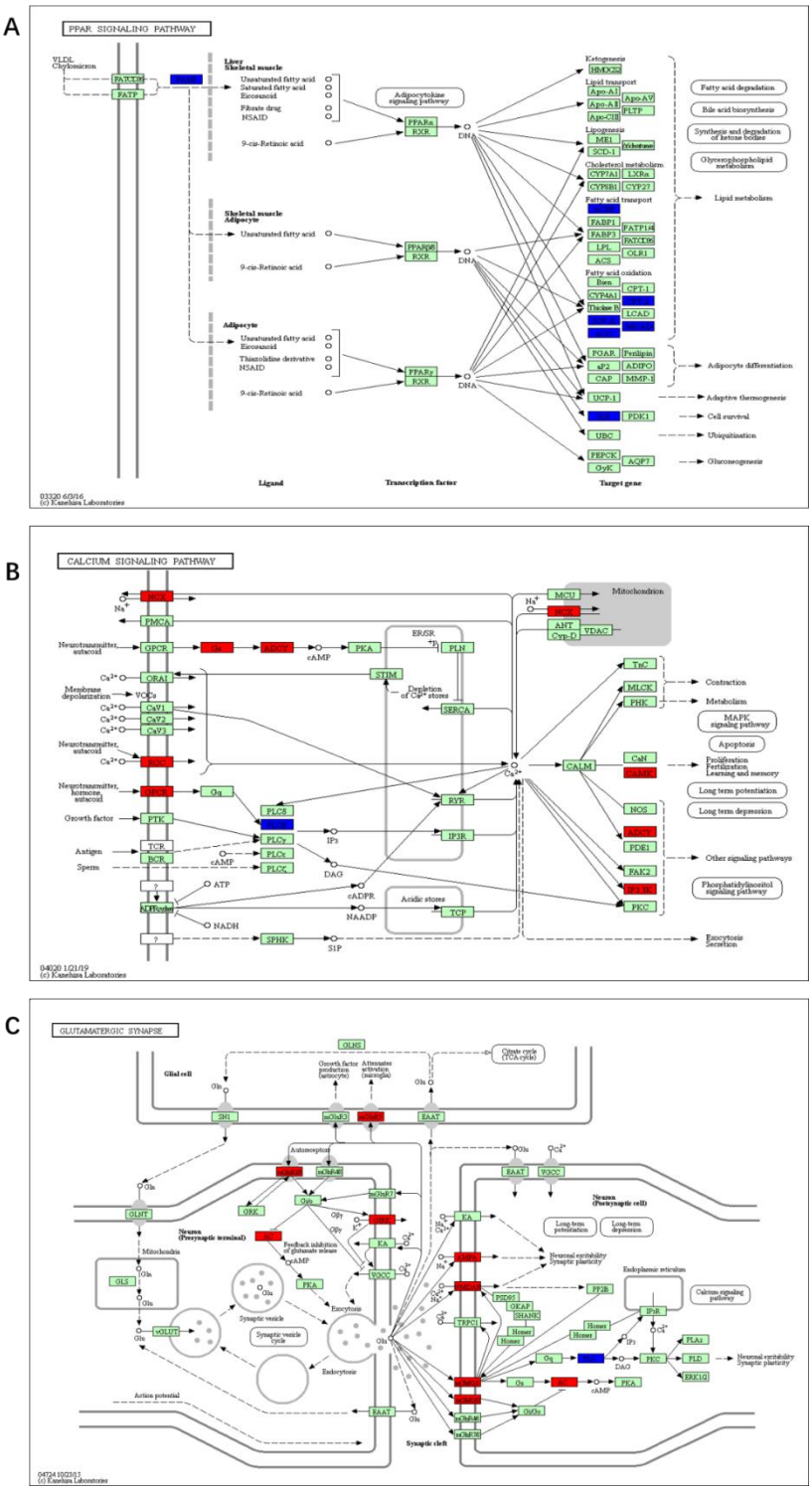

Additional Figure 3 Protein expression changes in PPAR signaling pathway (A), calcium signaling pathway (B) and glutamate synapse (C) between Tg + NSCs and Tg + PBS groups.

NSC transplantation leads to protein expression changes in PPAR, calcium and glutamate synapse pathways in Tg-tau mice compared to the Tg+PBS group. Red-colored box indicates upregulated proteins in pathways; blue-colored box indicates downregulated proteins in pathways; solid line indicates direct regulation; dashed line indicates indirect regulation. NSC: Neural stem cells; PBS: phosphate buffered saline; Tg: transgenic mice; PPAR: peroxisome proliferator-activated receptors. n = 3 for Tg + NSCs group; n = 3 for Tg + PBS group. The experiments were repeated by three times.

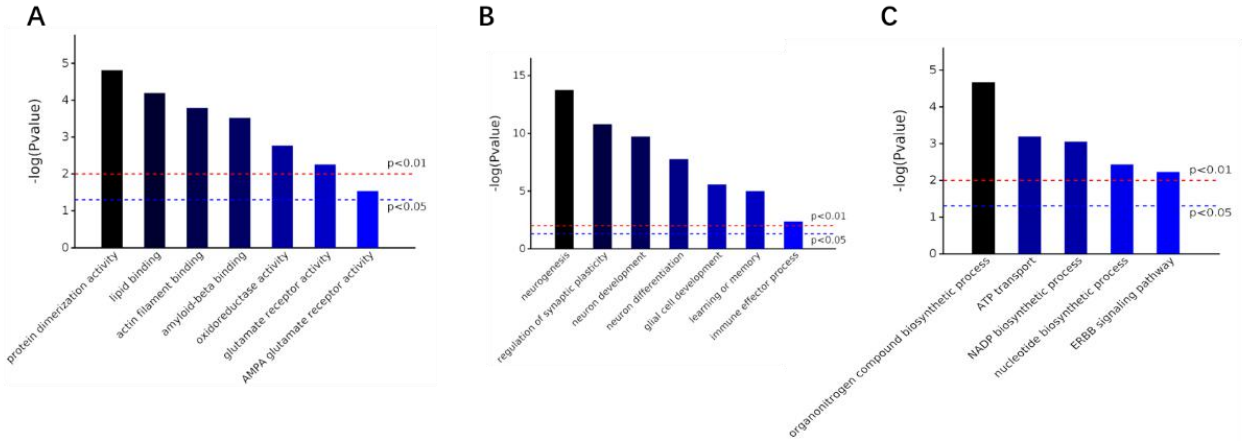

Additional Figure 4 Gene Ontology (GO) classifications of changed proteins with significance in certain pathways, including protein dimerization activity (A), neurogenesis (B), and biosynthetic process (C) between Tg + NSCs and Tg + PBS groups.

NSC transplantation leads to protein expression changes in certain pathways in Tg-tau mice compared to Tg + PBS group. *n* = 3 for Tg + NSCs group; *n* = 3 for Tg + PBS group. The experiments were repeated by three times.